

The Role of Hippocampal Iron Concentration and Hippocampal Volume in Age-Related Differences in Memory

Karen M. Rodrigue¹, Ana M. Daugherty², E. Mark Haacke³ and Naftali Raz²

¹School of Behavioral and Brain Sciences, Center for Vital Longevity, The University of Texas at Dallas, Dallas, TX, USA

²Department of Psychology, Institute of Gerontology and ³Department of Radiology, The MRI Institute for Biomedical Research, Wayne State University, Detroit, MI 48202, USA

Address correspondence to Karen M. Rodrigue. Email: krodrique@utdallas.edu

The goal of this study was to examine the relationships between 2 age-sensitive indices of brain integrity—volume and iron concentration—and the associated age differences in memory performance. In 113 healthy adults (age 19–83 years), we measured the volume and estimated iron concentration in the hippocampus (HC), caudate nucleus (Cd), and primary visual cortex (VC) in vivo with T2* relaxation times, and assessed memory performance with multiple tests. We applied structural equation modeling to evaluate the contribution of individual differences in 2 indices of integrity, volume and T2*, to age-related memory variance. The results show that in healthy adults, age differences in memory can be explained in part by individual differences in HC volume that in turn are associated with differences in HC iron concentration. Lower memory scores were linked to smaller HC and higher HC iron concentration. No such associations were noted for Cd and VC. We conclude that the association between age-related declines in memory and reduced hippocampal volume may reflect the impact of oxidative stress related to increase in free iron concentration. Longitudinal follow-up is needed to test whether altered iron homeostasis in the HC is an early marker for age-related cognitive decline.

Keywords: aging, brain, hippocampus, memory, T2*

Introduction

Reduced performance on tests of episodic memory accompanies advanced age (Craik 1977) and progressive deterioration of memory is the hallmark of cognitive disorders such as Alzheimer's disease (AD) (Katzman et al. 1988; Small et al. 2000). Although the neural mechanisms supporting memory formation and maintenance are manifold, and many brain structures contribute to memory formation and maintenance, one of its most prominent anatomical substrates is the hippocampus (HC) and adjacent structures that constitute the medial-temporal lobe (MTL, Squire 1987). Notably, the MTL is a brain area where Alzheimer type neuropathology appears at the earliest stages of the disease (Braak and Braak 1991). Even in normal adults, the HC shows significant shrinkage that accelerates around the sixth decade of life (e.g. Raz, Lindenberger et al. 2005, Raz, Ghisletta et al. 2010). Age-related differences in HC volume have been frequently, though not consistently, linked to poorer memory performance in healthy older adults (see Raz and Rodrigue 2006, Rodrigue and Kennedy 2011 for reviews), with the findings possibly limited by samples with a high representation of older participants (van Petten 2004).

As many aspects of brain structure and function change with age, it is plausible that, in addition to HC shrinkage, other physiological and metabolic factors play a role in

age-associated differences in memory. Among such factors, altered brain metabolism and accumulation of iron have recently received significant attention. Iron, which is essential for many cellular functions, presents in the brain in 2 major forms. First, heme iron constitutes the ferrous core of hemoglobin that binds oxygen and becomes paramagnetic when deoxygenated (Pauling and Coryell 1936). Deoxygenated heme iron contributes to local inhomogeneities that are detectable in magnetic resonance imaging (MRI) via differences in T2* relaxation times (Ogawa et al. 1990). The second form of brain iron is non-heme iron stored within the cerebral parenchyma to support normal metabolic function and neurotransmission (Mills et al. 2010). Intracellular non-heme iron (Fe²⁺ and Fe³⁺) is normally sequestered within ferritin (Schenck and Zimmerman 2004), which stabilizes the highly reactive ions. However, non-heme iron that escapes sequestration inflicts a significant negative effect on cellular integrity by promoting reactive oxygen species (Zecca et al. 2004; Mills et al. 2010). Iron-catalyzed oxidative stress is associated with aberrant dopamine and serotonin metabolism (Berg et al. 2007), differences in mitochondrial and nuclear DNA (Hamilton et al. 2001), and apoptosis (Zhang et al. 2009). For the lack of longitudinal studies, the life trajectory of brain iron concentration is unknown. However, numerous postmortem and cross-sectional in vivo studies have shown that in older brains, concentration of metabolically active iron particles increases in the cortical and, especially, subcortical gray matter (e.g. Hallgren and Sourander 1958; Bartzokis et al. 2007; see Haacke et al. 2005 for a review). An increased abundance of active iron is likely to promote oxidative stress and eventually, neurodegeneration, including the demyelination observed in healthy aging and its exacerbation in AD (Bartzokis 2011).

The importance of iron in brain aging and neurodegeneration makes the estimation of regional iron concentration of the brain in vivo highly desirable, and several methods have been proposed to attain that goal (Haacke et al. 2005; Pfefferbaum et al. 2009). One method is based on the calculation of the relaxation time constant that depends on the local inhomogeneities of the brain tissue: $1/T2^* = 1/T2 + 1/T2'$; (e.g. Ordidge et al. 1994; Martin et al. 1998; Shmueli et al. 2009; Yao et al. 2009). A strong link between shorter T2* and iron concentration and content of the parenchyma has been validated in postmortem and phantom studies (Thomas et al. 1993; Peran et al. 2009). T2*-based estimates of regional iron concentration revealed significant age-related differences in multiple regions (Raz, Rodrigue et al. 2007; Siemonsen et al. 2008; Cherubini et al. 2009; Rodrigue et al. 2011). T2* shortening has been reported in persons with hypertension (Rodrigue et al. 2011) and AD patients (Rombouts et al. 2007). Notably, whereas age-related differences in T2* and volume

of healthy adults are comparable in many brain regions, in the MTL structures, associations between T2* and age are significantly stronger than age differences in volume (Rodrigue et al. 2011).

Given the association of elevated brain iron with normal aging and age-related cognitive pathology, it is plausible that in healthy persons, age-related iron accumulation might be associated with reduced cognitive performance. To date, only a handful of studies have approached this question. Sullivan et al. (2009) previously reported significant associations of T2* values in the basal ganglia and thalamus with cognitive and motor performance. A more recent study reported that higher iron concentration in the HC was associated with significantly poorer recall in 33 older men (but not women), whereas increased iron in the basal ganglia was associated with poorer working memory (Bartzokis et al. 2011). Because the extant work is limited to middle aged and older adults, it remains unclear, whether the relationship between iron and cognition is limited to that part of the lifespan. Moreover, it is unclear, whether individual differences in the local brain iron concentration and regional volumes are related to cognitive performance. Although volumes and iron concentration have been measured in the same persons (Peran et al. 2009; Rodrigue et al. 2011), the conjoint impact of these indices of brain integrity on cognition is yet to be evaluated.

Therefore, the goal of the present study was to examine and compare the associations of local T2* (a proxy for iron concentration) and regional volume with memory performance in a large lifespan sample of healthy adults. Based on the previous findings of a stronger association between age and HC T2* in comparison to age differences in HC volume (Rodrigue et al. 2011), we hypothesized that individual differences in T2* would explain a greater share of age differences in an episodic memory than HC volumes would. We also tested the hypothesis that both indices of HC integrity would contribute independently to age-related memory variance. To evaluate the specificity of the putative associations of HC iron and volume with memory, we examined 2 additional regions of interests (ROIs). One region, the caudate nucleus (Cd), evidences age-related increases in the iron concentration comparable with those in the hippocampal formation; the other, primary visual (pericalcarine) cortex (VC), a control region that does not show significant age-related increases in iron concentration (Rodrigue et al. 2011).

Materials and Methods

Participants

The sample (described in detail in Rodrigue et al. 2011) consisted of 113 paid volunteers (76 women), age 19–83 years ($M = 53.96$, standard deviation [SD] = 15.39). None of the participants reported a history of cardiovascular, neurological or psychiatric disease, use of anti-seizure medication, anxiolytics, or antidepressants, head trauma with loss of consciousness for >5 min, thyroid problems, diabetes mellitus, or drug and alcohol problems. Persons with metal implants and dental prostheses that could affect image quality and T2* values were not included in the study. The participants had at least high school education, were native English speakers and consistent right-handers with Edinburgh Handedness Questionnaire (Oldfield 1971). To screen for dementia and

depression, we used the Mini-Mental State Examination (MMSE, Folstein et al. 1975; a cut-off of 26), and Center for Epidemiology Studies Depression Scale (CES-D, Radloff 1977; a cut-off of 15). The mean MMSE score was 28.62 ($SD = 1.12$) and the mean blood pressure values were 125.50 mmHg for systolic ($SD = 13.25$) and 77.25 mmHg for diastolic ($SD = 8.06$).

Seventeen participants who reported a diagnosis of hypertension were taking anti-hypertensive medications: calcium channel blockers—1 participant, angiotensin-converting enzyme inhibitors—2, angiotensin receptor II antagonist—1, beta-blockers—2, potassium-sparing diuretics—3, and 8 participants took a combination of at least 2 of these medications. The hypertensive participants were significantly older than their normotensive peers (61.65 vs. 52.59 years), $t = -3.11$, $P = 0.003$, but had a similar education level ($t = -1.18$, ns) and MMSE ($t(24) = -0.38$, ns). Mean systolic blood pressure for the hypertensive participants (137.85 mmHg) exceeded that of the normotensive participants (123.31 mmHg, $t = -5.16$, $P < 0.001$), as did diastolic pressure (81.09 vs. 76.57 mmHg, $t = -2.98$, $P = 0.005$), although both values were below the levels used in definition of hypertension (140/90 mmHg). All participants provided written informed consent at the beginning of the study and were debriefed after its completion.

Procedure

Blood Pressure Measurement

Blood pressure was measured by a mercury sphygmomanometer (Country Technology, Inc., Gays Mills, WI, USA; model 12–525) with a brachial cuff on 3 separate occasions in participants seated in a comfortable chair in a climate-controlled room. The values were averaged across occasions. Pulse pressure (mmHg) was calculated as the difference between the mean diastolic and the mean systolic pressures.

Memory Performance Measurement

To form a latent memory construct for the analyses reported below, we used immediate and delayed recall measures from memory for names and logical memory tests. Memory for names (subtest #1, Woodcock-Johnson Psychoeducational Battery-Revised, Woodcock and Johnson 1989) is a visual-auditory paired associate task. During acquisition, participants learn to associate a name with an image of an imaginary “space creature.” They first view a single space creature and are asked to point to the creature while the examiner repeats the associated name. The participants are asked to point to the just presented space creature and to the previously presented creature when the examiner names it. If the response is incorrect, the examiner provides corrective feedback. For the index of immediate memory (NamesI), correct responses are summed. There were 12 space creature stimuli and a maximum number correct response is 72. After a 20-min delay participants view pages with several space creatures and are asked to point to the creature named by the examiner. No corrections are given at that stage. Long-term recall (NamesL) is the total number of correct responses (maximum 36). The reliability of the memory for names indices is 0.91 (Woodcock and Johnson 1989).

In the logical memory test (Wechsler Memory Scale Revised, Wechsler 1987), participants listen to 2 paragraph-size stories, 1 at a time. Following each presentation, the

participants are asked to recall the story. They are also asked to recall the same stories, 1 at a time, after a 20-min delay. If a participant does not remember the story, a gist-based cue is provided by the examiner. Logical memory immediate (LMI) and delayed recall (LMD) indices of performance are the total number of correct details remembered for both stories (maximum 50).

MRI Acquisition Protocol

Images were acquired on a 1.5 T Siemens Sonata scanner. Regional T2* measurements were obtained from a multi-echo 3D Gradient-Recalled Echo (GRE) sequence with 48 axial slices, echo times (TE) = 10, 20, 30, 40, 50, 60, 70, and 80 ms; repetition time (TR) = 100 ms; field of view (FOV) = 256 × 256 mm²; bandwidth (BW) = 170 Hz/pixel, flip angle (FA) = 30°, and voxel size = 1 × 1 × 2 mm³. The 8-echo data were collected in a single high-BW sequence, which reduced problems associated with motion. Odd-number echoes were flow-compensated in the read direction. Sequence duration was 15:22 min. For regional volumetry, we acquired a magnetization prepared rapid acquisition gradient echo (MP-RAGE) sequence with 144 coronal slices, TE = 3.93 ms, TR = 800 ms, inversion time (TI) = 420 ms, FOV = 192 × 192 mm², BW = 130 Hz/pixel, acquisition matrix = 256 × 256, FA = 20°, and voxel size = 0.75 × 0.75 × 1.5 mm³. An 8-channel head coil was used for all sequences, thus considerably improving the signal to noise ratio.

T2 Relaxometry*

The raw data from the multi-echo GRE sequences were analyzed with locally designed software, Signal Processing in NMR (SPIN; MR Innovations, Inc., Detroit, MI, USA). Images were sorted by TE, and T2* maps were created by fitting the logarithm of the data for each echo on a pixel-by-pixel basis. We used a linear fit on the logarithm of the data, with the number of echoes varying from pixel to pixel depending on the local signal. To reduce error from field inhomogeneity, the signal from longer echoes that fell below 2 SDs of the noise was excluded from the fitting. The noise was calculated from 0.8 times the mean of the Rayleigh noise distribution. In a sub-sample, we confirmed that the error during linear fit did not differ between young ($n=5$, mean age of 20.40 years) and old ($n=5$, mean age of 78.80 years) participants across all ROIs. Average fit error in the HC (13.18 ± 1.36 and 12.26 ± 1.55 , young and old, respectively), Cd (11.03 ± 1.97 and 9.95 ± 1.47 , young and old, respectively), and VC (10.83 ± 1.15 and 10.62 ± 0.48 , young and old, respectively) did not differ by age ($0.38 < t < 1.0$, ns). Therefore, differences in the T2* calculation did not confound the individual measurements of regional T2*.

T2* values were sampled after interpolating the data by a factor of 2 in both in-plane dimensions of the transverse plane. The short-echo image (TE = 10 ms) was used to anatomically identify the ROIs. An oval-shaped probe the size of 24 contiguous pixels was placed within each ROI on the short TE image and copied onto the T2* map in the identical region to obtain the T2* mean and SD values. The operator placed the probe to exclude cerebral spinal fluid partial-voluming, major vasculature and potential microbleeds. Test-retest reliability (ICC3, ShROUT and Fleiss 1979) was assessed for 1 operator (K.M.R.) for each ROI on 10 images sampled twice with a 1-week delay and equaled at least 0.89.

Measurement of T2 per ROI*

The T2* values in the head of the HC were measured on 4 contiguous slices from the first slice on which it was apparent in the axial plane. This encompassed the extent of the anterior portion of the HC, which was chosen because of its reported sensitivity to aging (Hackert et al. 2002). HC T2* measurements (ICC(3) = 0.90) were obtained from the left and right hemispheres, separately and averaged. The T2* values for the Cd (ICC3 = 0.94) were measured on 4 consecutive axial slices from the first slices on which the structure appeared. The VC T2* was measured in the gray matter lining of the *calcarine sulcus* (ICC3 = 0.89) on 3 contiguous slices, beginning on the last slice, on which the superior colliculi remained visible. Because T2* is an estimate of the local iron content, and the probes were of a standard size, the recorded T2* values reflect relative iron concentration (content per unit of volume). It is important to note that although T2* values computed in this study are highly reliable and correlate highly with iron concentration values reported in the post-mortem literature (Rodrigue et al. 2011), the computed T2* is a relative index of iron burden. Whereas the region with shorter T2* contains more iron than a region with longer T2*, there is no precise translation between T2* (ms⁻¹) and absolute iron concentration (µg/g wet tissue).

Volumetry

The MP-RAGE images were reformatted to correct for head tilt, pitch, and rotation using the orthogonal tool in the Analyze software (Biomedical Imaging Resource, Mayo Clinic College of Medicine, Rochester, MN, USA). All images were aligned to be orthogonal to the long axis of the hippocampal formation. Aligned images were re-sliced into 0.5 × 0.5 × 0.5 mm³ contiguous sections. Images were displayed (magnified ×2) and traced manually with a stylus on a 21" LCD digitizing tablet (Wacom Cintiq 21UX). The ROIs were measured with the ROI tool in the Analyze software, and volumes were computed by multiplying the sum of areas by the slice thickness. Intracranial volume (ICV) was used to correct for differences in head and body size via a linear equation: $\text{Volume}_{\text{adj}i} = \text{Volume}_{\text{raw}i} - b(\text{ICV}_i - \text{Mean ICV})$ for each subject i . In this equation, $\text{Volume}_{\text{adj}i}$ is adjusted ROI volume, $\text{Volume}_{\text{raw}i}$ is the raw ROI volume, b is the slope of the ROI volume regression on ICV for the whole sample, and Mean ICV is the sample mean of the ICV. Reliability of the regional volumetric measures was assessed by an intraclass correlation coefficient, ICC(2) (presumption of random selection of raters; ShROUT and Fleiss 1979), equal to at least 0.90. HC volume was measured on a series of 19–25 slices, Cd on 15–20 slices, and VC on 15–18 slices. The auto-trace function in the Analyze program was used to measure the ICV with a reliability of ICC(2) = 0.99 and ICV did not vary by age ($\beta = 0.112$, $t(84) = 1.04$, ns). For details on the boundaries see Rodrigue et al. (2011).

Statistical Analysis

Structural equation modeling (SEM) with latent variables was implemented in Mplus (version 5.1, Muthen and Muthen, 2008). Prior to constructing latent variable models, all memory and anatomical measures were log-transformed to alleviate moderate skew. There were no sex differences in regional volumes adjusted for cranial size (all $F < 1$) or regional T2* values (the largest $F(1,110) = 1.61$, $P = 0.21$, ns.)

Therefore, observations from men and women were combined in the following analyses.

To avoid spurious results related to the modest sample size, all latent models were bootstrapped with a bias correction (500 iterations of the whole sample). To evaluate the specificity of the role of HC iron concentration and volume in age-related memory deficit, we tested 2 non-nested models: one that included Cd T2* and volume pathways as a plausible alternative and the other that included VC measures as a control comparison (Rodrigue et al. 2011). The relationships between pulse pressure and regional T2* and volume measures were also tested in these non-nested models. Following these analyses, nested models were constructed to test the hypothesized indirect association of age and memory through regional T2* and volume. Each model was reduced to exclude statistically non-significant pathways in order to standardized the magnitude beginning with the smallest value. After each reduction, the model was reassessed as the partial variance would be different and trending pathways might become significant.

Model fit was determined by multiple indices, including the normal theory weighted χ^2 statistic (a significant value indicates poor fit), the proportion of χ^2 to degrees of freedom (d.f.) (<2 indicates good fit), root mean square error of approximation (RMSEA, a value equal to or <0.05 indicates excellent fit), comparative fit and Tucker-Lewis fit indices (CFI and TLI, respectively, values exceeding 0.90 indicate excellent fit), standardized root mean residual (SRMR, <0.05 supports good fit), and Akaike and sample-size adjusted Bayesian information criteria (AIC and BIC, respectively, with comparatively smaller values indicating improved model fit) (Raykov and Marcoulides 2006). Because SEM is a confirmatory statistical technique, models were tested for the theoretical relationship between left and right measures within the regional T2* and volume constructs (Rodrigue et al. 2011). Indirect effects were evaluated according to the James and Brett (1984) method, in which a significant effect is sufficient to support an indirect relationship via the specified intermediate variable(s).

Table 1
Standardized measurement loading onto respective factors

Construct	Factor	Loading
Age	Mean-centered age	1.00 ^a
Pulse pressure	Average pulse pressure	1.00 ^a
HC T2*	Left HC T2*	0.58 ^a
	Right HC T2*	0.68*
HC volume	Left HC volume	0.79 ^a
	Right HC volume	0.85*
Cd T2*	Left Cd T2*	0.93 ^a
	Right Cd T2*	0.75*
Cd volume	Left Cd volume	0.98 ^a
	Right Cd volume	0.92*
VC T2*	Left VC T2*	0.35 ^a
	Right VC T2*	0.96*
VC volume	Left VC volume	1.00 ^a
	Right VC volume	0.23
Memory	Logical memory immediate	1.00 ^a
	Logical memory delayed	0.87*
	Memory for names immediate	0.87*
	Memory for names delayed	0.94*

^aFixed measurement error for latent scaling.

*Significant ($P < 0.05$) loading.

Results

Latent Factor Construction

Prior to model testing, a correlational latent variables model confirmed that all indicators represented the respective constructs (Table 1). To identify the Memory construct, immediate and delayed logical memory indices (LMI and LMD, respectively) were correlated with immediate (NamesI; standardized theta coefficient = -0.03 , $P < 0.05$, for each) and delayed (NamesD; standardized theta coefficients = -0.08 and -0.09 , $P < 0.05$, respectively) memory for names.

Zero-order correlations among the latent variables are presented in Table 2. Age and pulse pressure significantly correlated with all latent variables, except for VC T2* and volume. Age-related increase in regional iron concentration in the HC significantly correlated with HC volume (standardized path coefficient = 0.33 , $P < 0.05$), as did regional measures in the Cd (standardized path coefficient = 0.29 , $P < 0.05$). However, no association between regional iron concentration and volume was observed for the VC (Table 2).

Because a linear model analysis with age and sex as predictors of memory, HC volume, and HC T2* revealed neither sex differences nor age \times sex interactions (all $F < 1$), we did not include sex in the models. Collapsing the data over the sexes conserved degrees of freedom and allowed to avoid dealing with problematic dichotomous variables.

Hippocampal and Alternate ROI Model Comparisons

Non-nested models that compared HC against Cd and VC measures tested the hypothesized association of HC iron concentration and volume with age-related memory deficit. As shown in Figure 1, larger iron concentration in the Cd with advanced age (standardized coefficient = -0.56 , $P < 0.05$) associated with smaller volumes (standardized indirect effect = -0.13 , $P < 0.05$). Similarly, age was indirectly associated with smaller HC volume via increased regional iron concentration (standardized indirect effect = -0.31 , $P < 0.05$). Further, increased HC iron concentration and smaller volumes accounted for age-related memory deficits (standardized indirect effect = -0.09 , $P < 0.05$), whereas Cd measures did not (standardized indirect effect = 0.00 , $P = 0.74$).

Comparisons to the model including VC measures (Fig. 2) confirmed a significant indirect association of age with

Table 2
Correlations among latent constructs

	Age	Pulse pressure	HC T2*	HC volume	Cd T2*	Cd volume	VC T2*	VC volume
Pulse pressure	0.45*							
HC T2*	-0.62*	-0.35*						
HC volume	-0.24*	-0.21*	0.33*					
Cd T2*	-0.54*	-0.34*	0.43*	0.16				
Cd volume	-0.40*	-0.33*	0.22	0.41*	0.29*			
VC T2*	-0.14	-0.16	0.32	0.04	0.13	-0.01		
VC volume	-0.18	-0.18	0.41*	0.01	0.06	0.03	-0.04	
Memory	-0.23*	-0.21*	0.06	0.25*	0.27*	0.02	-0.04	0.25

Note: Regional T2* and volume and memory constructs are calculated as in the structural equation models.

*Significance at $P < 0.05$.

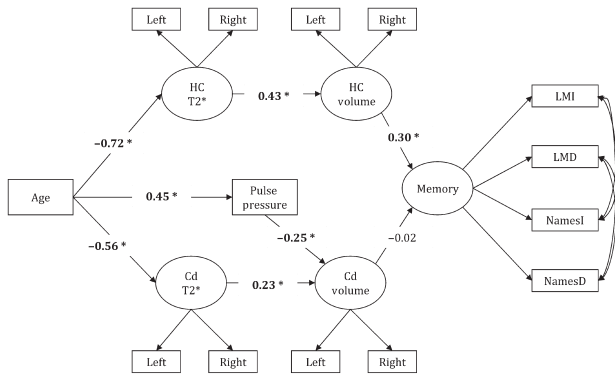


Figure 1. A model that tests Cd T2* and volume as alternate neural correlates of age-related memory deficits to HC measures. Abbreviations: Cd—caudate nucleus, LMI—logical memory, immediate recall; LMD—logical memory, delayed recall; NamesI—memory for names, immediate recall; NamesD—memory for names, delayed recall. Significant paths are shown in bold and * indicates significance at $P < 0.05$.

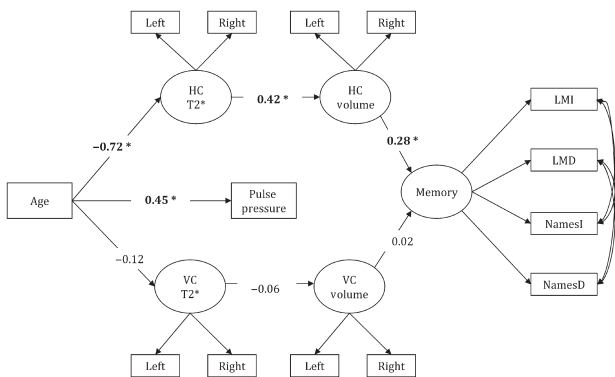


Figure 2. A model that tests VC T2* and volume associations with age-related memory deficits as a control comparison. Significant paths are shown in bold and * indicates significance, $P < 0.05$. Abbreviations: VC—primary visual cortex.

memory via HC T2* and volume differences (standardized indirect effect = -0.30 , $P < 0.05$) but not VC (standardized indirect effect = 0.01 , $P = 0.82$). All fit indices are shown in Table 3. A model comparing Cd and VC T2* and volumes in relation to age and memory performance did not converge for the lack of common variance.

The relation of memory performance to HC volume, HC iron concentration (T2*), and age is illustrated in Figure 3. The memory gradient surface shows that younger participants with larger hippocampi and lower HC iron concentration (longer T2*) had the highest memory composite scores. Moreover, the scatter plot shows that the observed association was not influenced by select cases.

Given that there was no association of Cd and VC measures with memory performance, we reduced the model to include only HC T2* and volume. Further, average pulse pressure was not significantly associated with HC measures or memory outcomes, and was therefore removed from the model. The associations between the left and right HC measures for both regional T2* and volume constructs were tested in the correlational model. Although the model fit well (Table 4), the correlational model would not converge if hemispheric HC measures were allowed to correlate, as would be expected on both statistical and theoretical grounds. Next, we examined

Table 3
Fit indices for the alternate ROI models

Index	Good fit ^a	HC and Cd*	HC and VC*
Nested models			
d.f.		65.0	65.0
χ^2		102.19	90.99
χ^2 P-value	> 0.05	0.01	0.03
χ^2 /d.f.	< 2	1.57	1.40
CFI	≥ 0.90	0.96	0.96
TLI	≥ 0.90	0.94	0.94
Non-nested models			
AIC	low value	312.53	2396.27
BIC	low value	457.08	2538.09
RMSEA	≤ 0.05	0.07	0.06
SRMR	≤ 0.05	0.11	0.10

Model includes correlation between the left and right measures for HC T2 and HC volume constructs.

^aRaykov and Marcoulides (2006).

Effect of age, hippocampal volume and hippocampal iron concentration on memory

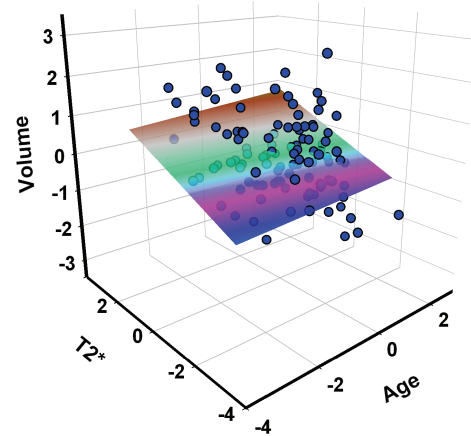


Figure 3. A scatter plot and memory performance gradient in the space of 3 predictors: age, HC iron concentration (T2*), and HC volume. Standardized (Z) scores are displayed on all axes. Higher scores indicate younger age, lesser iron concentration (longer T2*), and larger volume. The plane represents memory performance (latent composite scores) with brown indicating the highest and pink/purple the lowest scores.

models of direct age effects and various indirect effect models, including our hypothesized model, to explain variance in memory performance.

Direct and Indirect Age Effects

Direct Age Effects Model

The model of direct age effects on each variable of interest fit well (Table 4). Advanced age was associated with a significant increase in iron concentration inferred from T2* measures, decreased HC volume, and poorer memory performance (Fig. 4). However, if left and right HC T2* and volumetric measures were allowed to correlate, as would be plausibly expected, the model would not converge. Therefore, such model would be unrealistic and theoretically unsound.

Dual Indirect Paths Model

We tested an alternate model which predicted that age was indirectly associated with differences in memory through both decreased HC volume and increased regional iron

Table 4

Fit indices for all HC models

Index	Good fit ^a	Correlational model	Direct age effects	Dual indirect paths	Single indirect path A*	Single indirect path B	Reverse indirect effects
Nested models							
d.f.		23.00	28.00	29.00	27.00	29.00	29.00
χ^2		21.33	29.79	31.79	24.97	71.79	71.98
χ^2	>0.05	0.26	0.07	0.03	0.16	<0.0001	<0.0001
P-value							
χ^2 /d.f.	<2	1.19	1.49	1.67	1.31	3.42	3.43
CFI	≥ 0.90	0.99	0.98	0.97	0.99	0.89	0.89
TLI	≥ 0.90	0.99	0.96	0.95	0.98	0.82	0.82
Non-nested models							
AIC	low value	300.25	300.71	308.71	301.89	344.71	344.9
BIC	low value	398.44	387.99	404.17	397.35	434.71	434.9
RMSEA	≤ 0.05	0.04	0.07	0.08	0.05	0.15	0.15
SRMR	≤ 0.05	0.06	0.08	0.07	0.07	0.13	0.22

Model includes correlation between the left and right measures for HC T2 and HC volume constructs.

^aRaykov and Marcoulides (2006).

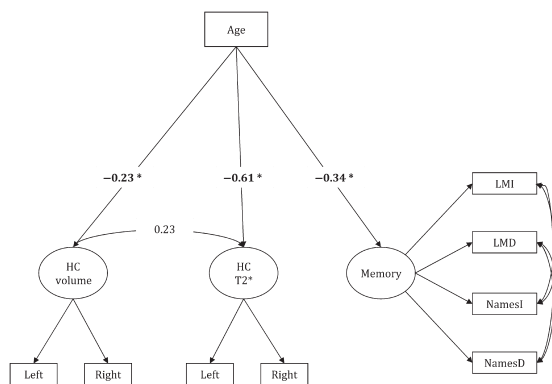


Figure 4. Direct age effects model. Significant paths are shown in bold and * indicates significance at $P < 0.05$.

concentration as separate paths (Fig. 5). The dual indirect paths model fit well (Table 4), but would not converge if left and right HC T2* and volumes were allowed to correlate. The assumption of independence of right and left hemispheric measures for both variables is highly unrealistic and, therefore, the model is unsuitable regardless of its fit to the data.

Single Indirect Path A and B Models

Our study hypothesis that the age-related differences in memory performance (low memory scores) are explained by individual differences in HC volume (smaller HC) via individual differences in HC iron concentration (greater HC iron concentration) was tested as model A (Fig. 6). The alternate hypothesis that age indirectly associated with increased HC iron concentration through a smaller HC volume was tested as model B (Supplementary Figure S1). Model A had excellent fit (Table 4) and included correlations between hemispheric measures of HC T2* and volume. In contrast, model B did not estimate correctly if left and right HC T2* measures were allowed to correlate, and thus was rejected on statistical and theoretical grounds (Table 4).

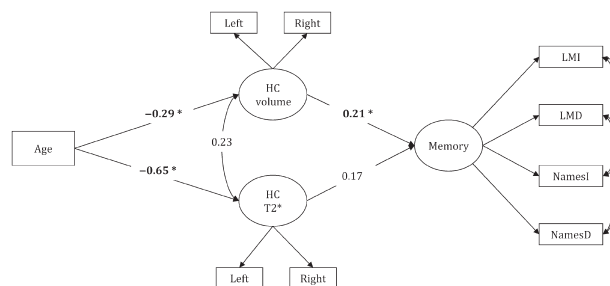


Figure 5. Dual indirect path model. Significant paths are shown in bold and * indicates significance at $P < 0.05$.

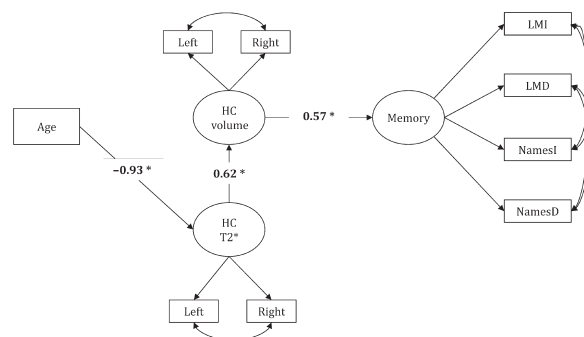


Figure 6. Single indirect path A model. Significant paths are shown in bold and * indicates significance at $P < 0.05$.

Reverse Indirect Effects Model

In a cross-sectional design, the indirect effects could be plausibly reversed: cognitive variables such as memory could explain the variance in brain indices through unspecified behavioral and lifestyle factors. However, the reverse indirect effects model did not fit well (Supplementary Figure S2 and Table 4), and would not converge if hemispheric HC T2* and volume measures were allowed to correlate, and was therefore rejected.

Thus, only hypothesized model A provided a theoretically plausible and statistically sound account of the observed variance in memory performance. This model supported a negative indirect association of age with HC volume through increased HC iron concentration (standardized indirect effect = -0.57 , $P < 0.0001$). In addition, advanced age was indirectly related to poorer memory performance through a shorter HC T2* and then smaller HC volume (standardized total indirect effect = -0.33 , $P < 0.0001$; Fig. 6).

Due to concerns about the use of anti-hypertension medication confounding the results, we assessed all models in the same sample after excluding 17 participants who used such prescriptions. The results did not change, except that the negative indirect association between age and memory performance via HC T2* and volume reached trend significance (standardized total indirect effect = -0.08 , $P = 0.06$).

Discussion

Our results demonstrate that age-related differences in memory performance are associated with at least 2 indices of hippocampal integrity: iron concentration and volume. These associations, however, are not independent. Age is associated

with significant decreases in T2* signal, interpreted as increases in iron concentration. Higher hippocampal iron is associated with smaller HC volume, which in turn predicted poorer memory performance. Thus, our findings suggest a specific age-related physiological mechanism for age-related differences in memory: accumulation of iron, an agent of oxidative stress.

The observed link between increased iron concentration and poorer memory is consistent with findings in animal models and humans. For example, in rodents, iron overload impairs spatial learning and memory (Maaroufi et al. 2009). A recent study reported an association between increased hippocampal ferritin and decreased word recall in a small sample of older men (Bartzokis et al. 2011). The present study demonstrates association between HC iron concentration and memory in a larger lifespan sample of healthy adults of both sexes. However, our results suggest that the negative association of iron concentration with memory may work indirectly through reduction in HC volume.

It is unclear if age-related increases in HC iron concentration reflect a normal aging process or represent an early physiological sign of impending pathological decline. Elevated iron levels have been reported in the HC of AD patients (Thompson et al. 1988) and impairment in homeostasis of iron (as well as other transition metals, such as copper and zinc) has been linked to oxidative stress (Deibel et al. 1996), a promoter of neurodegeneration. Iron accumulates in amyloid plaque in AD samples (Lovell et al. 1998; Collingwood et al. 2008) and has been observed within amyloid deposits in a transgenic mouse model of AD (Falangola et al. 2005). Moreover, elevated iron concentration is associated with lower MMSE scores in AD patients (Ding et al. 2009). Although the directionality of the link between amyloid and iron is unclear, existing evidence suggests that association between age and hippocampal T2* could reflect the underlying elevated beta-amyloid load.

Beta-amyloid is a key biomarker of AD pathology. It is elevated in approximately 20% of cognitively normal adults (Rowe et al. 2007; Price et al. 2009; see Rodrigue et al. 2009 for review), and amyloid burden correlates with reduced volume of multiple brain regions, including the HC (Chételat et al. 2010; Bourgeat et al. 2010). Notably, amyloid deposition that can be detected in healthy middle-aged adults may exert subtle negative effects on cognition (Rodrigue et al. 2012). Therefore, it is possible that fibrillar amyloid deposition, even in healthy adults, promotes regional brain atrophy and eventually results in cognitive decline (Jack et al. 2009). Testing a hypothesis regarding associations among HC iron, amyloid burden and volume is possible with a concurrent assessment of brain iron concentration and amyloid burden in vivo. However, the role of each of these factors in age-related cognitive decline can be established only in a longitudinal study.

Alternative interpretations of T2* shortening in the HC should be considered. It is possible that T2* decreases with age due to changes in brain vasculature. Differences in T2* may stem from alterations of cerebral microvascular dynamics and tissue oxygenation or from the changes in non-heme iron homeostasis. Age-related shortening of T2* could also reflect hemosiderin in cerebral microbleeds (CMB). Although CMB are relatively common among the general population of elderly (Greenberg et al. 2009), they are associated with less

than optimal cognitive status (Ayaz et al. 2010), and the likelihood of finding a significant CMB load in this optimally healthy sample with our T2* method is very low.

This study should be considered in the context of its limitations. First, the cross-sectional design precludes estimating change and drawing causal inferences. Secondly, by design, our sample consisted of healthy adults who, on average, had almost full college education. These characteristics limit generalization of findings to typical aging. Thirdly, our findings reflect an estimate of iron concentration in the anterior portion of the HC. The HC is a complex and non-uniform structure, and such regional estimate may not be representative of the entire hippocampal formation. Iron concentration could vary across the subsectors and along the long axis of the HC. Finally, our estimates of iron concentration were limited by a moderate field strength that may be insufficient for detection of subtle differences in T2* that are detectable with stronger magnets (Duyn et al. 2007, Shmueli et al. 2009). Thus, development of more precise methods of in vivo estimation of regional brain iron as well as the introduction of MRI scanners with higher field strength may help to elucidate the mechanisms that underpin the important age-related associations reported in this study.

In conclusion, the results of this study show that hippocampal iron concentration is negatively associated with memory performance in healthy adults. However, this association also depends upon an individual's HC volume. Our results suggest that altered iron homeostasis and the resulting elevation of oxidative stress may be a plausible biological modifier of hippocampal tissue loss and a harbinger of age-related cognitive decline. Although the longitudinal follow-up is necessary to test this hypothesis, within a given cross-sectional frame, older adults with smaller hippocampi and higher estimated iron concentration are likely to show poor performance on tests of episodic memory.

Supplementary Material

Supplementary material can be found at: <http://www.cercor.oxfordjournals.org/>.

Funding

This work was supported by the National Institutes of Health grants K99 AG-036848 to KR, R37 AG-011230 to NR, and training grant T32 HS-013819 to the Institute of Gerontology, Wayne State University.

Notes

Conflict of Interest: none declared.

References

- Ayaz M, Boikov AS, Haacke EM, Kido DK, Kirsch WM. 2010. Imaging cerebral microbleeds using susceptibility weighted imaging: one step toward detecting vascular dementia. *J Magn Reson Imaging.* 31:142–148.
- Bartzokis G. 2011. Alzheimer's disease as homeostatic responses to age-related myelin breakdown. *Neurobiol Aging.* 32:1341–1371.
- Bartzokis G, Lu P, Tingus K, Peters D, Amar CP, Tishler TA, Finn JP, Villablanca P, Alshuler LL, Mintz J et al. 2011. Gender and iron

- genes may modify associations between brain iron and memory in healthy aging. *Neuropsychopharmacology*. 36:1375–1384.
- Bartzokis G, Tishler T, Lu P, Villablanca P, Altshuler LL, Carter M, Huang D, Edwards N, Mintz J. 2007. Brain ferritin iron may influence age- and gender-related risks of neurodegeneration. *Neurobiol Aging*. 28:414–423.
- Berg D, Kruger R, RieB R, Riederer P. 2007. Parkinson's disease. In: Youdim M, Riederer P, Mandel S, Battistin L, editors. *Handbook of neurochemistry and molecular neurobiology: degenerative disease of the nervous system*. 3rd ed. New York (NY): Springer. p. 1–20.
- Bourgeat P, Chételat G, Villemagne VL, Fripp J, Raniga P, Pike K, Acosta O, Szoëke C, Ourselin S, Ames D. 2010. Beta-amyloid burden in the temporal neocortex is related to hippocampal atrophy in elderly subjects without dementia. *Neurology*. 74:121–127.
- Braak H, Braak E. 1991. Neuropathological staging of Alzheimer-related changes. *Acta Neuropathol*. 82:239–259.
- Cherubini A, Peran P, Caltagirone C, Sabatini U, Spalletta G. 2009. Aging of subcortical nuclei: microstructural, mineralization and atrophy modifications measured in vivo using MRI. *NeuroImage*. 48:29–36.
- Chételat G, Villemagne VL, Bourgeat P, Pike KE, Jones G, Ames D, Ellis KA, Szoëke C, Martins RN, O'Keefe GJ *et al.*; Australian Imaging Biomarkers and Lifestyle Research Group. 2010. Relationship between atrophy and β -amyloid deposition in Alzheimer disease. *Ann Neurol*. 67:317–324.
- Collingwood JF, Chong RK, Kasama T, Cervera-Gontard L, Dunin-Borkowski RE, Perry G, Pósfai M, Siedlak SL, Simpson ET, Smith MA *et al.* 2008. Three-dimensional tomographic imaging and characterization of iron compounds within Alzheimer's plaque core material. *J Alzheimers Dis*. 14:235–245.
- Craik FIM. 1977. Age differences in human memory. In: Birren JE, Schaie KW, editors. *Handbook of the psychology of aging*. New York (NY): Van Nostrand Reinhold. p. 384–420.
- Deibel MA, Ehmann WD, Markesbery WR. 1996. Copper, iron, and zinc imbalances in severely degenerated brain regions in Alzheimer's disease: possible relation to oxidative stress. *J Neurol Sci*. 143:137–142.
- Ding B, Chen K, Ling H, Sun F, Li X, Wan T, Chai WM, Zhang H, Zhan Y, Guan YJ. 2009. Correlation of iron in the hippocampus with MMSE in patients with Alzheimer's disease. *J Magn Reson Imaging*. 29:793–798.
- Duyn JH, van Gelderen P, Li TQ, de Zwart JA, Koretsky AP, Fukunaga M. 2007. High-field MRI of brain cortical substructure based on signal phase. *Proc Natl Acad Sci USA*. 104:11796–11801.
- Falangola MF, Lee SP, Nixon RA, Duff K, Helpert JA. 2005. Histological co-localization of iron in Abeta plaques of PS/APP transgenic mice. *Neurochem Res*. 20:201–205.
- Folstein M, Folstein S, McHugh P. 1975. "Mini-mental state." A practical method for grading the cognitive state of patients for the clinician. *J Psychiatr Res*. 12:189–198.
- Greenberg SM, Vernooij MW, Cordonnier C, Viswanathan A, Al-Shahi Salman R, Warach S, Launer LJ, Van Buchem MA, Breteler MM, Microbleed Study Group. 2009. Cerebral microbleeds: a guide to detection and interpretation. *Lancet Neurol*. 8:165–174.
- Haacke EM, Cheng NYC, House MJ, Liu Q, Neelavalli J, Ogg RJ, Khan A, Ayaz M, Kirsch W, Obenaus A. 2005. Imaging iron stores in the brain using magnetic resonance imaging. *Magn Reson Imaging*. 23:1–25.
- Hackert VH, den Haijer T, Oudkerk M, Koudstaal PJ, Hofman A, Breteler MM. 2002. Hippocampal head size associated with verbal memory performance in nondemented elderly. *NeuroImage*. 17:1365–1372.
- Hallgren B, Sourander P. 1958. The effect of age on the non-haem iron in the human brain. *J Neurochem*. 3:41–51.
- Hamilton M, Van Remmen H, Drake J, Yang H, Guo Z, Kewitt K, Walter C, Richardson A. 2001. Does oxidative damage to DNA increase with age? *Proc Natl Acad Sci*. 98:10469–10474.
- Jack CR, Jr, Lowe VJ, Weigand SD, Wiste HJ, Senjem ML, Knopman DS, Shiung MM, Gunter JL, Boeve BF, Kemp BJ. 2009. Serial PIB and MRI in normal, mild cognitive impairment and Alzheimer's disease: implications for sequence of pathological events in Alzheimer's disease. *Brain*. 132:1355–1365.
- James L, Brett J. 1984. Mediators, moderators, and test for mediation. *J Appl Psychol*. 69:307–321.
- Katzman R, Terry R, DeTeresa R, Brown T, Davies P, Fuld P, Renbing X, Peck A. 1988. Clinical, pathological, and neurochemical changes in dementia: a subgroup with preserved mental status and numerous neocortical plaques. *Ann Neurol*. 23:138–144.
- Lovell MA, Robertson JD, Teesdale WJ, Campbell JL, Markesbery WR. 1998. Copper, iron and zinc in Alzheimer's disease senile plaques. *J Neurol Sci*. 158:47–52.
- Maaroufi K, Ammari M, Jeljeli M, Roy V, Sakly M, Abdelmelek H. 2009. Impairment of emotional behavior and spatial learning in adult Wistar rats by ferrous sulfate. *Physiol Behav*. 96:343–349.
- Martin W, Ye F, Allen P. 1998. Increasing striatal iron content associated with normal aging. *Mov Disord*. 13:281–286.
- Mills E, Dong XP, Wang F, Xu H. 2010. Mechanisms of brain iron transport: insight into neurodegeneration and CNS disorders. *Future Med Chem*. 2:51–64.
- Ogawa S, Lee TM, Nayak AS, Glynn P. 1990. Oxygenation-sensitive contrast in magnetic resonance image of rodent brain at high magnetic fields. *Magn Reson Med*. 14:68–78.
- Oldfield R. 1971. The assessment and analysis of handedness. *Neuropsychologica*. 9:97–113.
- Ordidge R, Gorell J, Deniau J, Knight R, Helpert J. 1994. Assessment of relative brain iron concentrations using T2-weighted and T2*-weighted MRI at 3 tesla. *Magn Reson Med*. 32:335–341.
- Pauling L, Coryell CD. 1936. The magnetic properties and structure of hemoglobin, oxyhemoglobin and carbonmonoxyhemoglobin. *Proc Natl Acad Sci USA*. 22:210–216.
- Peran P, Cherubini A, Luccichenti G, Hagberg G, Demonet J, Rascol O, Celsis P, Caltagirone C, Spalletta G, Sabatini U. 2009. Volume and iron content in basal ganglia and thalamus. *Human Brain Mapp*. 30:2667–2675.
- Pfefferbaum A, Adalsteinsson E, Rohlfing T, Sullivan E. 2009. MRI estimates of brain iron concentration in normal aging: comparison of field-dependent (FDRI) and phase (SWI) methods. *NeuroImage*. 47:493–500.
- Price JL, McKeel DW, Jr, Buckles VD, Roe CM, Xiong C, Grundman M, Hansen LA, Petersen RC, Parisi JE, Dickson DW *et al.* 2009. Neuropathology of nondemented aging: presumptive evidence for preclinical Alzheimer disease. *Neurobiol Aging*. 30:1026–1036.
- Radloff L. 1977. The CES-D scale: a self-report depression scale for research in the general population. *J Struct Biol*. 153:42–54.
- Raykov T, Marcoulides G. 2006. *A first course in structural equation modeling*. 2nd ed. Mahwah, NJ: Lawrence Erlbaum.
- Raz N, Ghisletta P, Rodrigue K, Kennedy K, Lindenberger U. 2010. Trajectories of brain aging in middle-age and older adults: regional and individual differences. *NeuroImage*. 51:501–511.
- Raz N, Lindenberger U, Rodrigue KM, Kennedy KM, Head D, Williamson A, Dahle C, Gerstorf D, Acker JD. 2005. Regional brain changes in aging healthy adults: general trends, individual differences, and modifiers. *Cereb Cortex*. 15:1676–1689.
- Raz N, Rodrigue KM. 2006. Differential aging of the brain: patterns, cognitive correlates and modifiers. *Neurosci Biobehav Rev*. 30:730–748.
- Raz N, Rodrigue KM, Haacke EM. 2007. Brain aging and its modifiers: insights from in vivo neuromorphometry and susceptibility weighted imaging. *Ann N Y Acad Sci*. 1097:84–93.
- Rodrigue KM, Haacke EM, Raz N. 2011. Differential effects of age and history of hypertension on regional brain volumes and iron. *NeuroImage*. 54:750–759.
- Rodrigue KM, Kennedy KM. 2011. The cognitive consequences of structural changes to the aging brain. In: Schaie KW, Willis SL, editors. *Handbook of the psychology of aging*. 7th ed., Ch 5. New York (NY): Elsevier. p. 73–92.
- Rodrigue KM, Kennedy KM, Devous MD, Sr, Rieck JR, Hebrank AC, Diaz-Arrastia R, Mathews D, Park DC. 2012. β -amyloid deposition in healthy aging: regional deposition and cognitive consequences. *Neurology*. 78:387–395.

- Rodrigue KM, Kennedy KM, Park DC. 2009. Beta-amyloid deposition and the aging brain. *Neuropsychol Rev.* 19:436–450.
- Rombouts SA, Scheltens P, Kuijter JP, Barkhof F. 2007. Whole brain analysis of T2* weighted baseline fMRI signal in dementia. *Hum Brain Mapp.* 28:1313–1317.
- Rowe CC, Ng S, Ackermann U, Gong SJ, Pike K, Savage G, Cowie TF, Dickinson KL, Maruff P, Darby D *et al.* 2007. Imaging beta-amyloid burden in aging and dementia. *Neurology.* 68:1718–1725.
- Schenck JF, Zimmerman EA. 2004. High-field magnetic resonance imaging of brain iron: birth of a biomarker? *NMR Biomed.* 17:433–445.
- Shmueli K, de Zwart J, van Gelderen P, Li T-Q, Dodd SJ, Duyn JH. 2009. Magnetic susceptibility mapping of brain tissue in vivo using MRI phase data. *Magn Reson Med.* 62:1510–1522.
- Shrout P, Fleiss J. 1979. Intraclass correlations: uses in assessing raters reliability. *Psychol Bull.* 86:420–428.
- Siemonsen S, Finsterbusch J, Matschke J, Loerzen A, Ding X, Fiehler J. 2008. Age-dependent normal values of T2* and T2' in brain parenchyma. *Am J Neuroradiol.* 29:950–955.
- Small BJ, Fratiglioni L, Vitanen M, Winblad B, Backman L. 2000. The course of cognitive impairment in preclinical Alzheimer disease: three- and 6-year follow-up of a population-based sample. *Arch Neurol.* 57:839–844.
- Squire LR. 1987. *Memory and brain.* New York (NY): Oxford University Press.
- Sullivan EV, Adalsteinsson E, Rohling T, Pfefferbaum A. 2009. Relevance of iron deposition in deep gray matter brain structures to cognitive and motor performance in healthy elderly men and women: exploratory findings. *Brain Imaging Behav.* 3:167–175.
- Thomas L, Boyoko O, Anthony D, Burger P. 1993. MR detection of brain iron. *Am J Neuroradiol.* 14:1043–1048.
- Thompson CM, Markesbery WR, Ehmann WD, Mao YX, Vance DE. 1988. Regional brain trace-element studies in Alzheimer's disease. *Neurotoxicol.* 9:1–7.
- Van Petten C. 2004. Relationship between hippocampal volume and memory ability in healthy individuals across the lifespan: review and meta-analysis. *Neuropsychologia.* 42:1394–1413.
- Wechsler D. 1987. *Manual for Wechsler Memory Scale-Revised.* San Antonio (TX): Psychological Corporation.
- Woodcock RW, Johnson MB. 1989. *Woodcock-Johnson psycho-educational battery-revised.* Allen (TX): DLM Teaching Resources.
- Yao B, Li TQ, Gelderen P, Shmueli K, de Zwart JA, Duyn JH. 2009. Susceptibility contrast in high field MRI of human brain as a function of tissue iron content. *NeuroImage.* 44:1259–1266.
- Zecca L, Youdim MB, Riederer P, Connor JR, Crichton RR. 2004. Iron, brain ageing and neurodegenerative disorders. *Nat Rev Neurosci.* 5:863–873.
- Zhang S, Wang J, Song N, Xie J, Jiang H. 2009. Up-regulation of divalent metal transporter 1 is involved in 1-methyl-4-phenylpyridinium (MPP+)-induced apoptosis in MES23.5 cells. *Neurobiol Aging.* 30:1466–1476.